1 **Title:**

2 **Energetic Demands Regulate Sleep-Wake Rhythm Circuit Development**

3

4 **Authors:**

5 Amy R. Poe[1], Lucy Zhu[1], Si Hao Tang[1], Ella Valencia[1], Matthew S. Kayser[1,2,3*]

6

7 **Affiliations:**

8 1 Department of Psychiatry, Perelman School of Medicine, University of Pennsylvania,

9 Philadelphia, PA 19104, USA

10 2 Chronobiology and Sleep Institute, Perelman School of Medicine, University of

11 Pennsylvania, Philadelphia, PA 19104, USA

12 3 Department of Neuroscience, Perelman School of Medicine, University of

13 Pennsylvania, Philadelphia, PA 19104, USA

14

15 *Correspondence to: kayser@pennmedicine.upenn.edu

16

17 **Abstract:**

18 Sleep and feeding patterns lack a clear daily rhythm during early life. As diurnal animals

19 mature, feeding is consolidated to the day and sleep to the night. Circadian sleep

20 patterns begin with formation of a circuit connecting the central clock to arousal output

21 neurons; emergence of circadian sleep also enables long-term memory (LTM).

22 However, the cues that trigger the development of this clock-arousal circuit are

23 unknown. Here, we identify a role for nutritional status in driving sleep-wake rhythm

24   development in *Drosophila* larvae. We find that in the 2nd instar (L2) period, sleep and

25   feeding are spread across the day; these behaviors become organized into daily

26   patterns by L3. Forcing mature (L3) animals to adopt immature (L2) feeding strategies

27   disrupts sleep-wake rhythms and the ability to exhibit LTM. In addition, the development

28   of the clock (DN1a)-arousal (Dh44) circuit itself is influenced by the larval nutritional

29   environment. Finally, we demonstrate that larval arousal Dh44 neurons act through

30   glucose metabolic genes to drive onset of daily sleep-wake rhythms. Together, our data

31   suggest that changes to energetic demands in developing organisms triggers the

32   formation of sleep-circadian circuits and behaviors.

33

34   **Introduction**

35   The development of behavioral rhythms such as sleep-wake patterns is critical for brain

36   development[1]. Indeed, early life circadian disruptions in rodents negatively impacts

37   adult behaviors, neuronal morphology, and circadian physiology[2-4]. Likewise, in

38   humans, disruptions in sleep and rhythms during development are a common co-

39   morbidity in neurodevelopmental disorders including ADHD and autism[5-8]. Although the

40   molecular mechanisms encoding cellular rhythms are well understood, little is known

41   about how rhythmic behaviors first emerge[1,9-11]. In particular, the possible cues that

42   trigger the consolidation of sleep and waking behaviors as development proceeds are

43   unclear[12-15].

44   A key potential factor in the maturation of sleep patterns is the coincident change

45   in feeding and metabolism during development. Early in development, young animals

46   must obtain enough nutrients to ensure proper growth[16]. Yet, developing organisms

47   must also sleep to support nervous system development[1]. These conflicting needs

48   (feeding vs. quiescence) result in rapid transitions between sleeping and feeding states

49   early in life. As development proceeds, nutritional intake and storage capacity increase,

50   allowing for the consolidation of feeding and sleep to specific times of day. These

51   changes in nutritional storage capacity are likely conserved as mammalian body

52   composition and nutritional capacity changes over infant development[17] and *Drosophila*

53   show rapid increases in overall larval body size including the size of the fat body (used

54   for nutrient storage) across development[18,19]. However, the role that developmental

55   changes in metabolic drive plays in regulating the consolidation of behavioral rhythms is

56   not known.

57   In adult *Drosophila*, sleep and feeding behaviors are consolidated to specific

58   times of day with flies eating more in the day than the night[20]. Yet, early in development,

59   sleep in 2nd instar *Drosophila* larvae lacks a circadian pattern[21]. We previously

60   determined that sleep-wake rhythms are initiated in early 3rd instar *Drosophila* larvae

61   (L3) (72 hr AEL). DN1a clock neurons anatomically and functionally connect to Dh44

62   arousal output neurons to drive the consolidation of sleep in L3. Development of this

63   circuit promotes deeper sleep in L3 resulting in the emergence of long-term memory

64   (LTM) capabilities at the L3 stage but not before[21].

65   Here, we identify the cues that trigger the emergence of the DN1a-Dh44 circuit

66   and the consolidation of sleep-wake rhythms in *Drosophila* larvae. We demonstrate that

67   developmental changes to energetic demands drive consolidation of periods of sleep

68   and feeding across the day as animals mature. While endogenous deeper sleep in L3

69   facilitates LTM, we find that experimentally inducing deep sleep prematurely in (L2)

70   animals is detrimental to development and does not improve LTM performance.

71   Additionally, we demonstrate that DN1a-Dh44 circuit formation is developmentally

72   plastic, as rearing on an insufficient nutritional environment prevents establishment of

73   this neural connection. Finally, we find that Dh44 neurons require glucose metabolic

74   genes to promote sleep-wake rhythm development, suggesting that these neurons

75   sense the nutritional environment to promote circadian-sleep crosstalk.

76

77   **Results**

78   *Energetic demands limit developmental onset of rhythmic behaviors*

79   The emergence of circadian sleep-wake rhythms in *Drosophila* larvae is

80   advantageous as it enables long-term memory capabilities at the L3 stage. Yet, less

81   mature larvae do not exhibit consolidated sleep-wake patterns, prompting us to ask why

82   rhythmic behaviors do not emerge earlier in life. To determine if the absence of rhythmic

83   sleep-wake patterns in L2 might be related to feeding patterns, we examined larval

84   feeding rate (# mouth hook contractions in a 5-minute period) under constant conditions

85   at 4 times across the day (Circadian Time [CT] 1, CT7, CT13, and CT19) in

86   developmentally age-matched 2nd (L2) and early 3rd instar (L3; 72 hr AEL) larvae. While

87   we observed no differences in feeding rate across the day in L2, we found that L3 show

88   diurnal differences in feeding, specifically exhibiting a higher feeding rate during the

89   subjective light times compared to the subjective dark times (Figures 1A and 1B).

90   Analysis of total overall food intake indicates that L2 feed about the same at CT1 and

91   CT13; however, L3 at CT1 feed more than L3 at CT12 (Figure S1A). To assess whether

92   the daily pattern of feeding in early L3 is dependent on the canonical circadian biological

93   clock, we examined feeding rate in null mutants for the clock gene *tim*[22]. We observed

94   no differences in feeding rate across the day in *tim* mutants indicating that daily

95   changes in feeding rate require a functioning molecular clock at the L3 stage (Figure

96   1C). These findings underscore the tight relationship between sleep and feeding across

97   development as diurnal differences in sleep emerge concurrently at the L3 stage[21].

98   To further investigate how the emergence of circadian sleep is related to

99   changes in feeding patterns during development, we asked whether enforcing a

100   constant (immature) feeding pattern at the L3 stage affects sleep-wake rhythms. First,

101   we devised a nutritional paradigm with reduced sugar content but otherwise normal food

102   (low sugar, 1.2% glucose, L.S.). Critically, this paradigm did not affect any measures of

103   larval growth or development (Figures S1D-S1F). We found that the feeding pattern in

104   L3 raised on L.S. food closely resembled that of L2 on normal food (8% glucose) with

105   feeding spread out across the day (Figure 1D) (Figure S1A). Compared to L3 raised on

106   control food, this paradigm was also associated with loss of diurnal differences in sleep

107   duration, sleep bout number, and arousal threshold (Figures 1E and 1F) (Figures S1B

108   and S1C). Next, to avoid chronic effects of this manipulation, we acutely stimulated

109   feeding in L3 reared on normal food using thermogenetic activation of NPF+ neurons

110   (Figure 2A; Figure S2A)[23,24]. Like L.S. conditions, enforcing a constant feeding pattern

111   through NPF+ neuron activation led to loss of sleep rhythms and loss of deep sleep in

112   L3 (Figures 2B-2E; Figures S2B-S2E).

113   Disruption to circadian sleep and/or to deeper sleep stages during development

114   is associated with impairments in long-term memory formation[4,25-28]. We next asked if

115   the loss of deeper sleep observed in animals adopting a constant (strategic) feeding

116   strategy through either the L.S. paradigm or NPF+ neuron activation affects long-term

117   memory (LTM) capacity. Consistent with deeper sleep stages being necessary for LTM,

118   we observed a loss of LTM in either the NPF+ neuron activation (Figure 2F; Figures

119   S2F-2I) or under L.S. conditions (Figure 2H; Figures S1G-S1I). However, short-term

120   memory (STM) was intact in both manipulations (Figures 2G and 2I). These findings

121   suggest that immature feeding strategies preclude the emergence of sleep rhythms and

122   LTM. Altogether, our data indicate that consolidated periods of sleep and feeding

123   emerge due to developmentally dynamic changes in energetic demands.

124

125   *Deeper sleep stages are energetically disadvantageous in L2*

126   To investigate if promoting deep sleep at night in L2 can enable precocious LTM

127   abilities, we fed L2 larvae the GABA-A agonist gaboxadol[29,30]. While gaboxadol feeding

128   effectively induced deeper sleep in L2 (as reflected by an increase in arousal threshold),

129   LTM was still not evident (Figures 3A and 3B, 3E; Figures S3A and S3B); however, in

130   contrast to L3, L2 on gaboxadol failed to develop normally (Figures 3C and 3D). Next, to

131   avoid chronic pharmacological manipulations altogether, we acutely stimulated sleep-

132   inducing neurons using thermogenetics. We found that activation of these neurons

133   caused an increase in sleep amount and bout length with a decrease in arousal

134   threshold (Figures 3F and 3G; Figures S3C-S3H). However, inducing deeper sleep

135   stages in L2 did not improve LTM performance (Figure 3J; Figures S3I-S3K) despite

136   STM being intact (Figure S3L). Moreover, as with gaboxadol feeding in L2,

137   thermogenetic induction of deeper sleep stages disrupted larval development (Figures

138   3H and 3I). These data suggest that sleep cannot be leveraged to enhance cognitive

139 function prematurely because prolonged periods of deep sleep are not energetically

140 sustainable at this stage.

141

DN1a-Dh44 circuit formation is developmentally plastic

143 We previously determined that Dh44 arousal neurons anatomically and

144 functionally connect to DN1a clock neurons at the L3 stage[21]. Therefore, we examined

145 the functional connectivity between clock and arousal loci in the setting of nutritional

146 perturbation by expressing ATP-gated P2X2 receptors[31] in DN1a neurons and GCaMP6

147 in Dh44 neurons. As expected, activation of DN1as in L3 raised on control food caused

148 an increase in calcium in Dh44 neurons (Figures 4A and 4B)[21]. In contrast, in L3 raised

149 on L.S. conditions, activation of DN1as no longer elicited a response in Dh44 neurons

150 (Figures 4C and 4D). Thus, the nascent connection underlying circadian sleep in

151 *Drosophila* is developmentally plastic: in an insufficient nutritional environment, this

152 connection is not functional, facilitating a more constant feeding pattern that eschews

153 deep sleep at the expense of LTM.

154 We previously determined that release of *CCHamide-1* (*CCHa1*) from DN1as to

155 *CCHa1mide-1 receptor* (*CCHa1-R*) on Dh44 neurons is necessary for sleep-wake

156 rhythms in L3[21]. Although DN1as and Dh44 are not yet connected in L2, we next asked

157 whether Dh44 neurons in L2 are competent to receive the CCHa1 signal. CCHamide-1

158 peptide was bath applied onto dissected larval brains expressing *UAS-GCaMP7* in

159 Dh44 neurons. We observed an increase in intracellular calcium in early L3 (Figure 4F);

160 however, CCHa1 application did not alter calcium levels in Dh44 neurons in L2 (Figure

161 4E), indicating that Dh44 neurons are not capable of receiving CCHa1 input prior to

162 early L3. Surprisingly, CCHa1 application in L3 raised on L.S. also failed to elicit a

163 response in Dh44 neurons (Figure 4G) raising the possibility that sub-optimal nutritional

164 milieu influences the development of Dh44 neuronal competency to receive clock-driven

165 cues. Altogether, our data suggest that the nutritional environment influences DN1a-

166 Dh44 circuit development.

167

168 *Dh44 neurons require glucose metabolic genes to regulate sleep-wake rhythms*

169 How do developing larvae detect changes in their nutritional environments to

170 drive the circadian consolidation of sleep and feeding at the L3 stage? In adult

171 *Drosophila*, Dh44 neurons act as nutrient sensors to regulate food consumption and

172 starvation-induced sleep suppression through the activity of both glucose and amino

173 acid sensing genes[32-35]. We next asked whether Dh44 neurons in L3 require metabolic

174 genes to regulate sleep-wake rhythms. We conducted an RNAi-based candidate screen

175 in L3 raised on control food of different glucose and amino acid sensing genes known to

176 act in adult Dh44 neurons. Sleep duration at CT1 and CT13 was assessed with

177 knockdown of glucose metabolic genes (*Hexokinase-C*, *Glucose transporter 1,* and

178 *Pyruvate kinase*) or amino acid sensing genes (*Gcn2* and its downstream target ATF4

179 or *cryptocephal*) in Dh44 neurons. We found that knockdown of glucose metabolism

180 genes, *Glut1*, *Hex-C* and *PyK*, in Dh44 neurons resulted in a loss of rhythmic changes

181 in sleep duration and bout number (Figures 5A-5C; Figures S4A-S4F) with no effect on

182 L3 feeding in the *Hex-C* manipulation (Figure 5D). Manipulation of glucose metabolic

183 genes in L2 did not affect sleep duration at CT1 and CT13 (Figures 5E-5G; Figures

184 S4G-S4L) providing evidence that nutrient sensing is not required at this stage to

185   regulate sleep. In contrast to their role in adult Dh44 neurons, knockdown of amino acid

186   sensing genes, *Gcn2* and *crc*, in Dh44 neurons did not disrupt rhythmic changes in

187   sleep duration and bout number in L3 (Figures 5H and 5I; Figures S4M-S4P)

188   suggesting that Dh44 neurons may not act through amino acid sensing pathways to

189   regulate sleep-wake rhythm development. Thus, Dh44 neurons require glucose

190   metabolic genes to drive sleep-wake rhythm development. Our data indicate that the

191   emergence of diurnal behavioral differences such as sleep-wake is driven by

192   developmental changes in energetic capacity and suggest that Dh44 neurons may be

193   necessary for sensing of larval nutritional environments.

194

195   **Discussion**

196   Nutritional environment and energetic status exert profound effects on sleep

197   patterns during development, but mechanisms coupling sleep to these factors remain

198   undefined. We report that the development of sleep-circadian circuits depends on

199   organisms achieving sufficient nutritional status to support the consolidation of deep

200   sleep at night. In contrast to their role in adult flies, our data demonstrate that larval

201   Dh44 neurons act through glucose metabolic genes but not amino acid sensing genes

202   to modulate sleep-wake rhythms. This suggests that larval Dh44 neurons may have

203   distinct functions from their adult counterparts for integrating information about the

204   nutritional environment through the direct sensing of glucose levels to modulate sleep-

205   wake rhythm development. Maintaining energy homeostasis and sensing of the

206   nutritional environment are likely conserved regulators of sleep-wake rhythm

207   development as young mice exposed to a maternal low-protein diet show disruptions in

208   night-time sleep architecture and energy expenditure later in life[36,37].

209   Together with our previously published work, our findings support a model in

210   which changes in both overall circuit development and molecular changes in post-

211   synaptic (Dh44) neurons likely drive sleep-wake rhythm circuit development. Our

212   CCHa1 peptide data suggest that Dh44 neurons may undergo changes in CCHa1-R

213   expression or subcellular localization between the L2 and L3 stages; we only observed

214   an increase in Dh44 neural activity in response to the bath application of CCHa1

215   peptide at the L3 stage (Figures 4E and 4F). Interestingly, this increase in activity is lost

216   in low nutrient conditions (Figure 4G) suggesting that the larval nutritional environment

217   may also modulate CCHa1-R localization or expression. Indeed, we observed a

218   disruption of sleep rhythms in L3 when glucose metabolic genes are knocked down in

219   Dh44 neurons demonstrating that post-synaptic changes likely initiate onset of circadian

220   sleep. These findings raise intriguing questions for how changes in an organism's

221   energetic and nutritional state influence sleep-circadian circuit development. Perhaps

222   larval Dh44 neurons respond to an increase in glucose levels in the environment by

223   promoting CCHa1-R localization to the membrane. In this model, changes in CCHa1-R

224   subcellular localization allow Dh44 neurons to become competent to receive clock-

225   driven cues, while this or other Dh44-derived signals promote circuit connectivity with

226   DN1as to drive consolidation of sleep at the L3 stage. There are no available

227   endogenous fluorescent reporters of CCHa1-R, limiting our ability to examine receptor

228   subcellular localization. Nevertheless, our data provide exciting avenues of future work

229   on the molecular and subcellular mechanisms regulating DN1a-Dh44 circuit

230   development.

231   Our data demonstrate that larvae exhibit both sleep-wake and feeding rhythms at

232   the L3 stage, but not earlier[21]. This raises the obvious question of whether sleep and

233   feeding are opposite sides of the same coin. While larvae cannot eat when they are

234   sleeping, we have observed distinct effects of certain manipulations on sleep behaviors

235   but not feeding. For example, knockdown of *Hex-C* in Dh44 neurons disrupts sleep

236   rhythms with no obvious effect on feeding behavior (Figure 5D). Moreover, preliminary

237   data suggests that manipulating possible feeding-rhythmic relevant circuitry disrupts

238   feeding rhythms with no apparent effect on sleep-wake rhythms (data not shown). It is,

239   of course, possible to affect both sleep and feeding behaviors with the same circuit

240   manipulation indicating that they are also inter-connected behaviors. For example,

241   thermogenetic activation of NPF+ neurons causes an increase in feeding rate while also

242   causing a decrease in sleep duration. Future work will leverage the larval system to

243   examine how sleep-wake and feeding circuitry communicate to balance these two

244   behaviors across developmental periods.

245

246   **Acknowledgements:**

254

Author contributions:

256 Conceptualization, A.R.P., M.S.K.; Investigation, A.R.P., L.Z., S.H.T., E.V.; Writing –

257 Original Draft, A.R.P. and M.S.K.; Writing – Review & Editing, all authors; Project

258 supervision and funding, M.S.K.

259

260 **Data and Materials Availability**: All data needed to evaluate the conclusions in the

261 paper are present in the paper and/or the Supplementary Materials.

262

263 **Competing Interests:** All authors declare that they have no competing interests.

264

265 **Materials and Methods**

266 **Fly Stocks**

267 The following lines have been maintained as lab stocks or were obtained from Dr. Amita

268 Sehgal: iso31, tim0[22], Dh44[VT]-Gal4 (VT039046)[38], cry-Gal4 pdf-Gal80[39], UAS-TrpA1[40],

269 UAS-mCherry RNAi, LexAOP-GCaMP6 UAS-P2X2[31], and UAS-GCaMP7f. Dh44-LexA

270 (80703), npf-Gal4 (25681), R76G11-Gal4 (48333), Hex-C RNAi (57404), Glut1 RNAi

271 (40904), PyK RNAi (35218), GCN2 RNAi (67215), and crc RNAi (80388) were from the

272 Bloomington *Drosophila* Stock Center (BDSC).

273

Larval rearing and sleep assays

Larval sleep experiments were performed as described previously[21,41]. Briefly, molting

2nd instar or 3rd instar larvae were placed into individual wells of the LarvaLodge

containing either 120 µl (for L2) or 95 µl (for L3) of 3% agar and 2% sucrose media

covered with a thin layer of yeast paste. The LarvaLodge was covered with a

transparent acrylic sheet and placed into a DigiTherm (Tritech Research) incubator at

25°C for imaging. Experiments were performed in the dark. For thermogenetic

experiments, adult flies were maintained at 22°C. Larvae were then placed into the

LarvaLodge (as described above) which was moved into a DigiTherm (Tritech

Research) incubator at 30°C for imaging.

LarvaLodge image acquisition and processing

Images were acquired every 6 seconds with an Imaging Source DMK 23GP031 camera

(2592 X 1944 pixels, The Imaging Source, USA) equipped with a Fujinon lens

(HF12.55A-1, 1:1.4/12.5 mm, Fujifilm Corp., Japan) with a Hoya 49mm R72 Infrared

Filter as described previously[21,41]. We used IC Capture (The Imaging Source) to acquire

time-lapse images. All experiments were carried out in the dark using infrared LED

strips (Ledlightsworld LTD, 850 nm wavelength) positioned below the LarvaLodge.

Images were analyzed using custom-written MATLAB software (see Churgin et al

2019[42] and Szuperak et al 2018[41]). Temporally adjacent images were subtracted to

generate maps of pixel value intensity change. A binary threshold was set such that

individual pixel intensity changes that fell below 40 gray-scale units within each well

297   were set equal to zero ("no change") to eliminate noise. For 3rd instars, the threshold

298   was set to 45 to account for larger body size. Pixel changes greater than or equal to

299   threshold value were set equal to one ("change"). Activity was then calculated by taking

300   the sum of all pixels changed between images. Sleep was defined as an activity value

301   of zero between frames. For 2nd instar sleep experiments done across the day, total

302   sleep was summed over 6 hrs beginning 2 hrs after the molt to second instar. For sleep

303   experiments performed at certain circadian times, total sleep in the 2nd hour after the

304   molt to second (or third) instar was summed.

305

306   **Feeding behavior analysis**

307   For feeding rate analysis, newly molted 2nd instar or 3rd instar larvae were placed in

308   individual wells of the LarvaLodge containing 120 µl of 3% agar and 2% sucrose media

309   covered with a thin layer of yeast paste. Larvae were then imaged continuously with a

310   Sony HDR-CX405 HD Handycam camera (B&H Photo, Cat. No: SOHDRCX405) for 5

311   minutes. The number of mouth hook contractions (feeding rate) was counted manually

312   over the imaging period and raw numbers were recorded. For food intake analysis,

313   newly molted 2nd instar or 3rd instar larvae were starved for 1 hr in petri dishes with

314   water placed on a Kimwipe. To compare groups of larvae of similar body weights, 13 L3

315   larvae and 26 L2 larvae were grouped together. Larvae were placed in a petri dish

316   containing blue-dyed 3% agar, 2% sucrose, and 2.5% apple juice with blue-dyed yeast

317   paste on top for 4 hrs at 25°C in constant darkness. After 4 hrs, groups of larvae were

318   washed in water, put in microtubes, and frozen at -80°C for 1 hr. Frozen larvae were

319   then homogenized in 300 µl of distilled water and spun down for 5 min at 13,0000 rpm.

320   The amount of blue dye in the supernatant was then measured using a

321   spectrophotometer (OD_{629}). Food intake represents the OD value of each

322   measurement.

323

324   **Aversive Olfactory conditioning**

325   We used an established two odor reciprocal olfactory conditioning paradigm with 10 mM

326   quinine (quinine hydrochloride, EMSCO/Fisher, Cat. No: 18-613-007) as a negative

327   reinforcement to test short-term or long-term memory performance in L2 and early L3

328   larvae[43] at CT12-15[21]. Experiments were conducted on assay plates (100 X 15 mm,

329   Genesee Scientific, Cat. No: 32-107) filled with a thin layer of 2.5% agarose containing

330   either pure agarose (EMSCO/Fisher, Cat. No: 16500-500) or agarose plus reinforcer.

331   As olfactory stimuli, we used 10 µl amyl acetate (AM, Sigma-Aldrich, Cat. No:

332   STBF2370V, diluted 1:50 in paraffin oil-Sigma-Aldrich, Cat. No: SZBF140V) and octanol

333   (OCT, Fisher Scientific, Cat. No: SALP564726, undiluted). Odorants were loaded into

334   the caps of 0.6 mL tubes (EMSCO/Fisher, Cat. No: 05-408-123) and covered with

335   parafilm (EMSCO/Fisher, Cat. No: 1337412). For naïve preferences of odorants, a

336   single odorant was placed on one side of an agarose plate with no odorant on the other

337   side. A group of 30 larvae were placed in the middle. After 5 minutes, individuals were

338   counted on the odorant side, the non-odorant side, or in the middle. The naïve

339   preference was calculated by subtracting the number of larvae on the non-odorant side

340   from the number of larvae on the odorant side and then dividing by the total number of

341   larvae. For naïve preference of quinine, a group of 30 larvae were placed in the middle

342   of a half agarose-half quinine plate. After 5 minutes, individuals were counted on the

343   quinine side, the agarose side, or in the middle. The naïve preference for quinine was

344   calculated by subtracting the number of larvae on the quinine side from the number of

345   larvae on the agarose side and then dividing by the total number of larvae. Larvae were

346   trained by exposing a group of 30 larvae to AM while crawling on agarose medium plus

347   quinine reinforcer. After 5 min, larvae were transferred to a fresh Petri dish containing

348   agarose alone with OCT as an odorant (AM+/OCT). A second group of 30 larvae

349   received the reciprocal training (AM/OCT+). Three training cycles were used for all

350   experiments. For long-term memory, larvae were transferred after training onto agarose

351   plates with a small piece of Kimwipe moistened with tap water and covered in dry active

352   yeast (LabScientific, Cat. No: FLY804020F). Larvae were then kept in the dark for 1.5

353   hrs before testing memory performance. Training and retention for thermogenetic

354   experiments were conducted at 30°C. For short-term memory, larvae were immediately

355   transferred after training onto test plates (agarose plus reinforcer) on which AM and

356   OCT were presented on opposite sides of the plate. After 5 min, individuals were

357   counted on the AM side, the OCT side, or in the middle. We then calculated a

358   preference index (PREF) for each training group by subtracting the number of larvae on

359   the conditioned stimulus side from the number of larvae on the unconditioned stimulus

360   side. For one set of experiments, we calculated two PREF values: 1a) $PREF_{AM+/OCT}$ =

361   (#AM - #OCT)/ # TOTAL; 1b) $PREF_{AM/OCT+}$ = (#OCT-#AM)/ # TOTAL. We then took the

362   average of each PREF value to calculate an associative performance index (PI) as a

363   measure of associative learning. PI = $(PREF_{AM+/OCT}$ + $PREF_{AM/OCT+})$/2.

364

365   **Arousal threshold**

366 Blue light stimulation was delivered as described in [21,41] using 2 high power LEDs

367 (Luminus Phatlight PT-121, 460 nm peak wavelength, Sunnyvale, CA) secured to an

368 aluminum heat sink. The LEDs were driven at a current of 0.1 A (low intensity). We

369 used a low intensity stimulus for 4 sec every 2 minutes for 1 hr beginning the 2nd hr after

370 the molt to second (or third) instar. We then counted the number of larvae that showed

371 an activity change in response to stimulus. The percentage of animals that moved in

372 response to the stimulus was recorded for each experiment. For each genotype, at least

373 4 biological replicates were performed. We then plotted the average percentage across

374 all replicates.

375

376 **P2X2 Activation and GCaMP imaging**

377 All live imaging experiments (P2X2 and CCHa1 bath application) were performed as

378 described previously[21]. Briefly, brains were dissected in artificial hemolymph (AHL)

379 buffer consisting of (in mM): 108 NaCl, 5 KCl, 2 CaCl2, 8.2 MgCl2, 4 NaHCO3, 1

380 NaH2PO4-H20, 5 Trehalose, 10 Sucrose, 5 HEPES, pH=7.5. Brains were placed on a

381 small glass coverslip (Carolina Cover Glasses, Circles, 12 mm, Cat. No: 633029) in a

382 perfusion chamber filled with AHL.

383   For P2X2 imaging, dissections were performed at CT12-15 and AHL buffer was

384 perfused over the brains for 1 min of baseline GCaMP6 imaging, then ATP was

385 delivered to the chamber by switching the perfusion flow from the channel containing

386 AHL to the channel containing 2.5 mM ATP in AHL, pH 7.5. ATP was perfused for 2 min

387 and then AHL was perfused for 2 min. Twelve-bit images were acquired with a 40 X

388 water immersion objective at 256 X 256-pixel resolution. Z-stacks were acquired every 5

389   sec for 3 min. Image processing and measurement of fluorescence intensity was

390   performed in ImageJ as described previously[21]. For each cell body, fluorescence traces

391   over time were normalized using this equation: $\Delta F/F = (F_n-F_0)/F_0$, where

392   F_n=fluorescence intensity recorded at time point n, and F_0 is the average fluorescence

393   value during the 1 min baseline recording. Maximum GCaMP change ($\Delta F/F$) for

394   individual cells was calculated using this equation: $\Delta F/F_{max} = (F_{max}-F_0)/F_0$, where

395   F_{max}=maximum fluorescence intensity value recorded during ATP application, and F_0 is

396   the average fluorescence value during the 1 min baseline recording. All analysis was

397   done blind to experimental condition.

398   For CCHa1 bath application, dissections were performed at CT12-15 and AHL

399   buffer was perfused over the brains for 1 min of baseline GCaMP7f imaging, then

400   CCHa1 peptide was delivered to the chamber by switching the perfusion flow from the

401   channel containing AHL to the channel containing 1 µM synthetic CCHa1 in AHL, pH

402   7.5. CCHa1 was perfused for 2 min, followed by a 1 min wash-out with AHL. For the

403   AHL negative control, the perfusion flow was switched from one channel containing AHL

404   to another channel containing AHL. Twelve-bit images were acquired with a 40 X water

405   immersion objective at 256 X 256-pixel resolution. Z-stacks were acquired every 10 sec

406   for 4 min. Image processing and measurement of fluorescence intensity was performed

407   in ImageJ. A max intensity Z-projection of each time step and Smooth thresholding was

408   used for analysis. Image analysis was performed in a similar manner as for the P2X2

409   experiments. All analysis was done blind to experimental condition.

410

411   **Gaboxadol treatment**

412 Early second or third instar larvae were starved for 1 hour and then fed 75 µl of 25

413 mg/mL Gaboxadol (hydrochloride) (Thomas Scientific, Cat No: C817P41) in diluted

414 yeast solution for 1 hour prior to loading in LarvaLodge containing 120 µl of 3% agar

415 and 2% sucrose media covered with a thin layer of 25 mg/mL Gaboxadol yeast paste.

416 For LTM experiments, starved early second instars were fed 25 mg/mL Gaboxadol for 1

417 hour prior to training and maintained on 25 mg/mL Gaboxadol in diluted yeast solution

418 during retention period.

419

420 **Dietary Manipulations**

421 Fly food was prepared using the following recipes (based on Poe et al 2020)[44]:

Ingredients	Control food (444 mM glucose)	Low sugar (L.S.) (66 mM glucose)
Distilled H_2O	234 mL	234 mL
Agar	2 g (10g/L)	2 g (10g/L)
Glucose	20 g	3 g
Inactive yeast	20 g	20 g
Acid mix (phosphoric acid + propionic acid)	2 mL	2 mL
Target final solution volume	250 mL	250 mL

422

423   Acid Mix was made by preparing Solution A (41.5 ml Phosphoric Acid mixed with 458.5

424   ml distilled water) and Solution B (418 ml Propionic Acid mixed with 82 ml distilled

425   water) separately and then mixing Solution A and Solution B together.

426   Adult flies were placed in an embryo collection cage (Genesee Scientific, cat#: 59-100)

427   and eggs were laid on a petri dish containing either control (ctrl) or Low sugar (L.S.)

428   food. Animals developed on this media for three days.

429

430   **Larval Body Weight and Length Measurements**

431   For weight, groups of 5 early 3rd instar larvae raised on either control- or low sugar

432   (L.S.)-filled petri dishes were washed in tap water and dried using a Kimwipe. The 5

433   larvae were then weighed as a group on a scale and the weight in mg was recorded.

434   For the Gaboxadol experiments, groups of 10 early 2nd instar larvae or groups of 5 early

435   3rd instar larvae were weighed. For length, images of individual early 3rd instar larvae in

436   the LarvaLodge were measured in ImageJ (Fiji) using the straight line tool. The total

437   body length was determined in pixels for individual larvae on each condition.

438

439   **Statistical analysis**

440   All statistical analysis was done in GraphPad (Prism). For comparisons between 2

441   conditions, two-tailed unpaired t-tests were used. For comparisons between multiple

442   groups, ordinary one-way ANOVAs followed by Tukey's multiple comparison tests were

443   used. For comparisons between different groups in the same analysis, ordinary one-

444   way ANOVAs followed by Sidak's multiple comparisons tests were used. For

445   comparisons between time and genotype, two-way ANOVAs followed by Sidak's

446   multiple comparisons tests were used. For comparison of GCaMP signal in CCHa1

447   experiments, Mann-Whitney test was used. *P<0.05, **P<0.01, ***P<0.001.

448   Representative confocal images are shown from at least 8-10 independent samples

449   examined in each case.

450

451   **References**

452   1.   Vallone, D., Lahiri, K., Dickmeis, T., and Foulkes, N.S. (2007). Start the clock!
453   Circadian rhythms and development. Dev Dyn *236*, 142-155. 10.1002/dvdy.20998.
454   2.   Varcoe, T.J., Voultsios, A., Gatford, K.L., and Kennaway, D.J. (2016). The impact of
455   prenatal circadian rhythm disruption on pregnancy outcomes and long-term metabolic
456   health of mice progeny. Chronobiol Int *33*, 1171-1181.
457   10.1080/07420528.2016.1207661.
458   3.   Mendez, N., Halabi, D., Spichiger, C., Salazar, E.R., Vergara, K., Alonso-Vasquez, P.,
459   Carmona, P., Sarmiento, J.M., Richter, H.G., Seron-Ferre, M., and Torres-Farfan, C.
460   (2016). Gestational Chronodisruption Impairs Circadian Physiology in Rat Male
461   Offspring, Increasing the Risk of Chronic Disease. Endocrinology *157*, 4654-4668.
462   10.1210/en.2016-1282.
463   4.   Ameen, R.W., Warshawski, A., Fu, L., and Antle, M.C. (2022). Early life circadian
464   rhythm disruption in mice alters brain and behavior in adulthood. Sci Rep *12*, 7366.
465   10.1038/s41598-022-11335-0.
466   5.   Hoffmire, C.A., Magyar, C.I., Connolly, H.V., Fernandez, I.D., and van Wijngaarden, E.
467   (2014). High prevalence of sleep disorders and associated comorbidities in a community
468   sample of children with Down syndrome. J Clin Sleep Med *10*, 411-419.
469   10.5664/jcsm.3618.
470   6.   Krakowiak, P., Goodlin-Jones, B., Hertz-Picciotto, I., Croen, L.A., and Hansen, R.L.
471   (2008). Sleep problems in children with autism spectrum disorders, developmental
472   delays, and typical development: a population-based study. J Sleep Res *17*, 197-206.
473   10.1111/j.1365-2869.2008.00650.x.
474   7.   Kotagal, S. (2015). Sleep in Neurodevelopmental and Neurodegenerative Disorders.
475   Semin Pediatr Neurol *22*, 126-129. 10.1016/j.spen.2015.03.003.
476   8.   Ednick, M., Cohen, A.P., McPhail, G.L., Beebe, D., Simakajornboon, N., and Amin, R.S.
477   (2009). A review of the effects of sleep during the first year of life on cognitive,
478   psychomotor, and temperament development. Sleep *32*, 1449-1458.
479   10.1093/sleep/32.11.1449.
480   9.   Carmona-Alcocer, V., Abel, J.H., Sun, T.C., Petzold, L.R., Doyle, F.J., 3rd, Simms, C.L.,
481   and Herzog, E.D. (2018). Ontogeny of Circadian Rhythms and Synchrony in the
482   Suprachiasmatic Nucleus. J Neurosci *38*, 1326-1334. 10.1523/JNEUROSCI.2006-
483   17.2017.

484   10.   Sehgal, A., Price, J., and Young, M.W. (1992). Ontogeny of a biological clock in
485   Drosophila melanogaster. Proc Natl Acad Sci U S A *89*, 1423-1427.
486   10.1073/pnas.89.4.1423.
487   11.   Poe, A.R., Mace, K.D., and Kayser, M.S. (2021). Getting into rhythm: developmental
488   emergence of circadian clocks and behaviors. FEBS J. 10.1111/febs.16157.
489   12.   Blumberg, M.S., Seelke, A.M., Lowen, S.B., and Karlsson, K.A. (2005). Dynamics of
490   sleep-wake cyclicity in developing rats. Proc Natl Acad Sci U S A *102*, 14860-14864.
491   10.1073/pnas.0506340102.
492   13.   Blumberg, M.S., Gall, A.J., and Todd, W.D. (2014). The development of sleep-wake
493   rhythms and the search for elemental circuits in the infant brain. Behav Neurosci *128*,
494   250-263. 10.1037/a0035891.
495   14.   Frank, M.G., Ruby, N.F., Heller, H.C., and Franken, P. (2017). Development of
496   Circadian Sleep Regulation in the Rat: A Longitudinal Study Under Constant Conditions.
497   Sleep *40*. 10.1093/sleep/zsw077.
498   15.   Frank, M.G. (2020). The Ontogenesis of Mammalian Sleep: Form and Function. Curr
499   Sleep Med Rep *6*, 267-279. 10.1007/s40675-020-00190-y.
500   16.   Ghosh, S., Korte, A., Serafini, G., Yadav, V., and Rodenfels, J. (2023). Developmental
501   energetics: Energy expenditure, budgets and metabolism during animal embryogenesis.
502   Semin Cell Dev Biol *138*, 83-93. 10.1016/j.semcdb.2022.03.009.
503   17.   Toro-Ramos, T., Paley, C., Pi-Sunyer, F.X., and Gallagher, D. (2015). Body composition
504   during fetal development and infancy through the age of 5 years. Eur J Clin Nutr *69*,
505   1279-1289. 10.1038/ejcn.2015.117.
506   18.   Butterworth, F.M., Emerson, L., and Rasch, E.M. (1988). Maturation and degeneration of
507   the fat body in the Drosophila larva and pupa as revealed by morphometric analysis.
508   Tissue Cell *20*, 255-268. 10.1016/0040-8166(88)90047-x.
509   19.   Jacobs, H.T., George, J., and Kemppainen, E. (2020). Regulation of growth in Drosophila
510   melanogaster: the roles of mitochondrial metabolism. J Biochem *167*, 267-277.
511   10.1093/jb/mvaa002.
512   20.   Barber, A.F., Erion, R., Holmes, T.C., and Sehgal, A. (2016). Circadian and feeding cues
513   integrate to drive rhythms of physiology in Drosophila insulin-producing cells. Genes
514   Dev *30*, 2596-2606. 10.1101/gad.288258.116.
515   21.   Poe, A.R., Zhu, L., Szuperak, M., McClanahan, P.D., Anafi, R.C., Scholl, B., Thum,
516   A.S., Cavanaugh, D.J., and Kayser, M.S. (2023). Developmental emergence of sleep
517   rhythms enables long-term memory in Drosophila. Sci Adv *9*, eadh2301.
518   10.1126/sciadv.adh2301.
519   22.   Konopka, R.J., and Benzer, S. (1971). Clock mutants of Drosophila melanogaster. Proc
520   Natl Acad Sci U S A *68*, 2112-2116. 10.1073/pnas.68.9.2112.
521   23.   Wu, Q., Wen, T., Lee, G., Park, J.H., Cai, H.N., and Shen, P. (2003). Developmental
522   Control of Foraging and Social Behavior by the Drosophila Neuropeptide Y-like System.
523   Neuron *39*, 147-161. 10.1016/s0896-6273(03)00396-9.
524   24.   Chung, B.Y., Ro, J., Hutter, S.A., Miller, K.M., Guduguntla, L.S., Kondo, S., and
525   Pletcher, S.D. (2017). Drosophila Neuropeptide F Signaling Independently Regulates
526   Feeding and Sleep-Wake Behavior. Cell Rep *19*, 2441-2450.
527   10.1016/j.celrep.2017.05.085.

25. Konrad, C., Seehagen, S., Schneider, S., and Herbert, J.S. (2016). Naps promote flexible memory retrieval in 12-month-old infants. Dev Psychobiol *58*, 866-874. 10.1002/dev.21431.

26. Seehagen, S., Konrad, C., Herbert, J.S., and Schneider, S. (2015). Timely sleep facilitates declarative memory consolidation in infants. Proc Natl Acad Sci U S A *112*, 1625-1629. 10.1073/pnas.1414000112.

27. Jones, C.E., Opel, R.A., Kaiser, M.E., Chau, A.Q., Quintana, J.R., Nipper, M.A., Finn, D.A., Hammock, E.A.D., and Lim, M.M. (2019). Early-life sleep disruption increases parvalbumin in primary somatosensory cortex and impairs social bonding in prairie voles. Sci Adv *5*, eaav5188. 10.1126/sciadv.aav5188.

28. Smarr, B.L., Grant, A.D., Perez, L., Zucker, I., and Kriegsfeld, L.J. (2017). Maternal and Early-Life Circadian Disruption Have Long-Lasting Negative Consequences on Offspring Development and Adult Behavior in Mice. Sci Rep *7*, 3326. 10.1038/s41598-017-03406-4.

29. Dissel, S., Angadi, V., Kirszenblat, L., Suzuki, Y., Donlea, J., Klose, M., Koch, Z., English, D., Winsky-Sommerer, R., van Swinderen, B., and Shaw, P.J. (2015). Sleep restores behavioral plasticity to Drosophila mutants. Curr Biol *25*, 1270-1281. 10.1016/j.cub.2015.03.027.

30. Dijk, D.J., Stanley, N., Lundahl, J., Groeger, J.A., Legters, A., Trap Huusom, A.K., and Deacon, S. (2012). Enhanced slow wave sleep and improved sleep maintenance after gaboxadol administration during seven nights of exposure to a traffic noise model of transient insomnia. J Psychopharmacol *26*, 1096-1107. 10.1177/0269881111421971.

31. Yao, Z., Macara, A.M., Lelito, K.R., Minosyan, T.Y., and Shafer, O.T. (2012). Analysis of functional neuronal connectivity in the Drosophila brain. J Neurophysiol *108*, 684-696. 10.1152/jn.00110.2012.

32. Dus, M., Lai, J.S., Gunapala, K.M., Min, S., Tayler, T.D., Hergarden, A.C., Geraud, E., Joseph, C.M., and Suh, G.S. (2015). Nutrient Sensor in the Brain Directs the Action of the Brain-Gut Axis in Drosophila. Neuron *87*, 139-151. 10.1016/j.neuron.2015.05.032.

33. Yang, Z., Huang, R., Fu, X., Wang, G., Qi, W., Mao, D., Shi, Z., Shen, W.L., and Wang, L. (2018). A post-ingestive amino acid sensor promotes food consumption in Drosophila. Cell Res *28*, 1013-1025. 10.1038/s41422-018-0084-9.

34. Oh, Y., Lai, J.S., Min, S., Huang, H.W., Liberles, S.D., Ryoo, H.D., and Suh, G.S.B. (2021). Periphery signals generated by Piezo-mediated stomach stretch and Neuromedin-mediated glucose load regulate the Drosophila brain nutrient sensor. Neuron *109*, 1979-1995 e1976. 10.1016/j.neuron.2021.04.028.

35. Oh, Y., and Suh, G.S.B. (2023). Starvation-induced sleep suppression requires the Drosophila brain nutrient sensor. J Neurogenet, 1-8. 10.1080/01677063.2023.2203489.

36. Sutton, G.M., Centanni, A.V., and Butler, A.A. (2010). Protein malnutrition during pregnancy in C57BL/6J mice results in offspring with altered circadian physiology before obesity. Endocrinology *151*, 1570-1580. 10.1210/en.2009-1133.

37. Crossland, R.F., Balasa, A., Ramakrishnan, R., Mahadevan, S.K., Fiorotto, M.L., and Van den Veyver, I.B. (2017). Chronic Maternal Low-Protein Diet in Mice Affects Anxiety, Night-Time Energy Expenditure and Sleep Patterns, but Not Circadian Rhythm in Male Offspring. PLoS One *12*, e0170127. 10.1371/journal.pone.0170127.

572   38.   Jenett, A., Rubin, G.M., Ngo, T.T., Shepherd, D., Murphy, C., Dionne, H., Pfeiffer, B.D.,
573   Cavallaro, A., Hall, D., Jeter, J., et al. (2012). A GAL4-driver line resource for
574   Drosophila neurobiology. Cell Rep *2*, 991-1001. 10.1016/j.celrep.2012.09.011.
575   39.   Stoleru, D., Peng, Y., Agosto, J., and Rosbash, M. (2004). Coupled oscillators control
576   morning and evening locomotor behaviour of Drosophila. Nature *431*, 862-868.
577   10.1038/nature02926.
578   40.   Hamada, F.N., Rosenzweig, M., Kang, K., Pulver, S.R., Ghezzi, A., Jegla, T.J., and
579   Garrity, P.A. (2008). An internal thermal sensor controlling temperature preference in
580   Drosophila. Nature *454*, 217-220. 10.1038/nature07001.
581   41.   Szuperak, M., Churgin, M.A., Borja, A.J., Raizen, D.M., Fang-Yen, C., and Kayser, M.S.
582   (2018). A sleep state in Drosophila larvae required for neural stem cell proliferation.
583   eLife *7*. 10.7554/eLife.33220.
584   42.   Churgin, M.A., Szuperak, M., Davis, K.C., Raizen, D.M., Fang-Yen, C., and Kayser,
585   M.S. (2019). Quantitative imaging of sleep behavior in Caenorhabditis elegans and larval
586   Drosophila melanogaster. Nat Protoc *14*, 1455-1488. 10.1038/s41596-019-0146-6.
587   43.   Widmann, A., Artinger, M., Biesinger, L., Boepple, K., Peters, C., Schlechter, J., Selcho,
588   M., and Thum, A.S. (2016). Genetic Dissection of Aversive Associative Olfactory
589   Learning and Memory in Drosophila Larvae. PLoS Genet *12*, e1006378.
590   10.1371/journal.pgen.1006378.
591   44.   Poe, A.R., Xu, Y., Zhang, C., Lei, J., Li, K., Labib, D., and Han, C. (2020). Low FoxO
592   expression in Drosophila somatosensory neurons protects dendrite growth under nutrient
593   restriction. Elife *9*. 10.7554/eLife.53351.
594
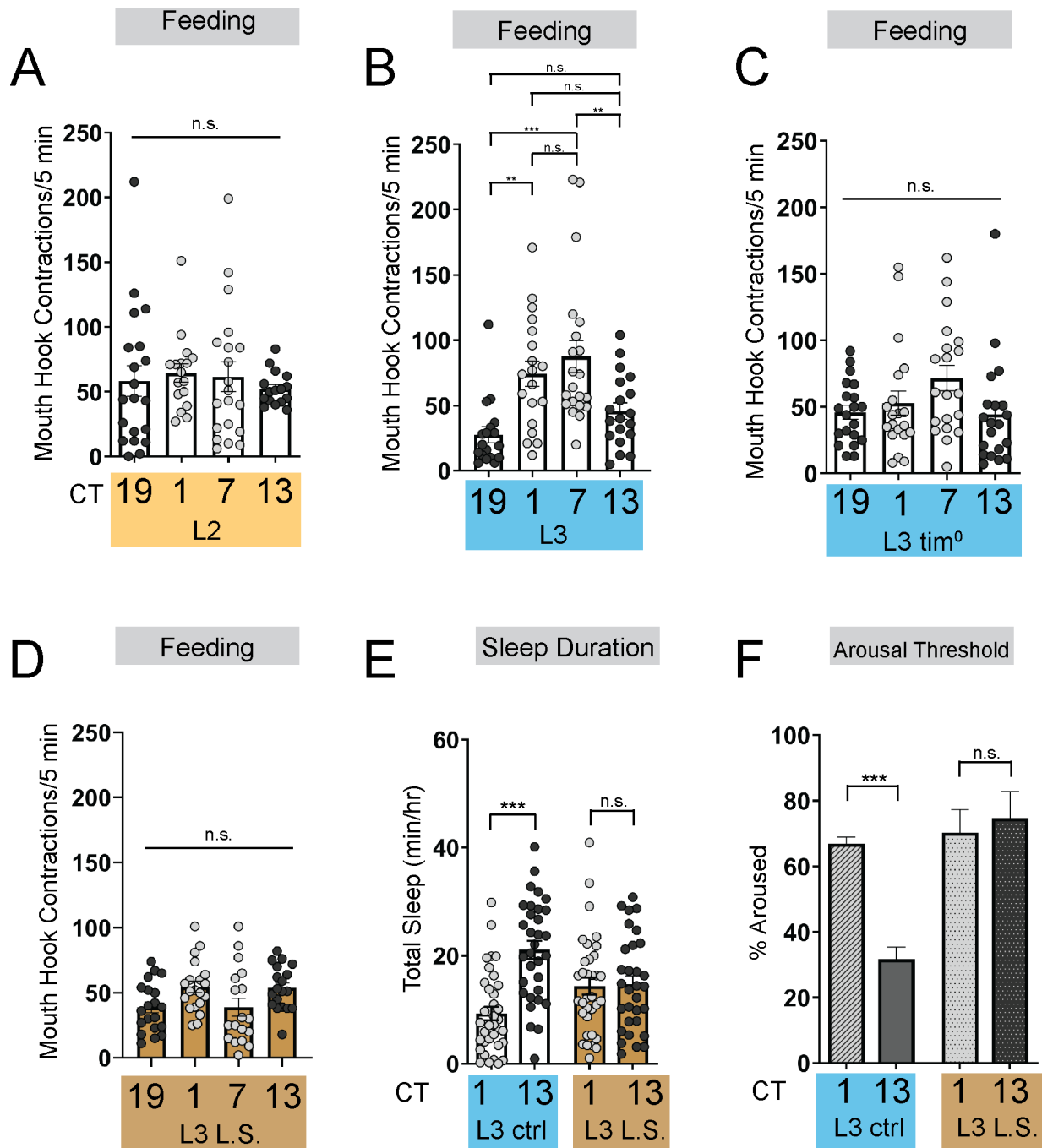
Figure 1: Energetic drive limits sleep rhythm development
(A-D) Feeding rate (# of mouth hook contractions per 5 min) of L2 controls (A), L3 raised on regular (ctrl) food (B), L3 clock mutants (C), and L3 raised on low sugar (L.S.) food (D) across the day. **(E)** Sleep duration at CT1 and CT13 in L3 raised on regular (ctrl) and L.S. food. **(F)** Arousal threshold at CT1 and CT13 in L3 raised on regular (ctrl) and L.S. food. A-D, n=18-20 larvae; E, n=29-34 larvae; F, n= n=100-172 sleep episodes, 18 larvae per genotype. One-way ANOVAs followed by Sidak's multiple comparisons tests [(A-D)]; Two-way ANOVAs followed by Sidak's multiple comparison test [(E-F)]. For

this and all other figures unless otherwise specified, data are presented as mean ± SEM; n.s., not significant, *P<0.05, **P<0.01, ***P<0.001.
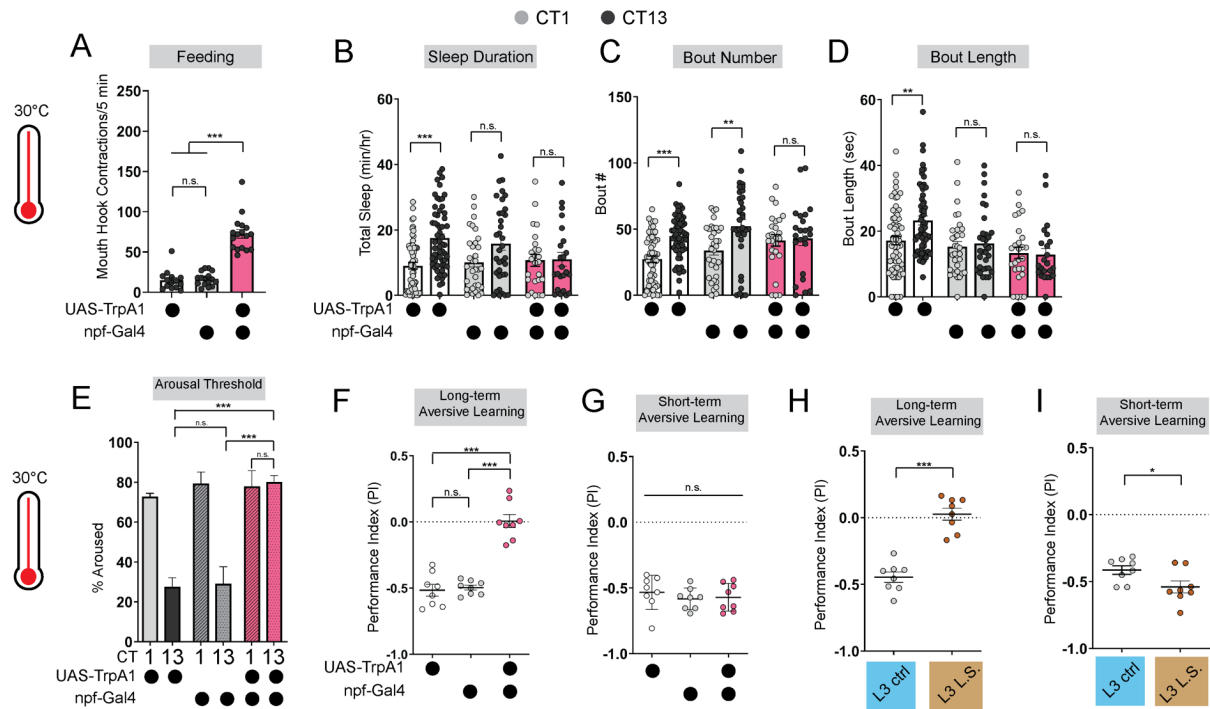
Figure 2: Immature feeding strategies perturb LTM performance.
(A) Feeding rate of L3 expressing *npf*-Gal4>*UAS-TrpA1* and genetic controls at 30°C at CT13. **(B-D)** Sleep duration (B), bout number (C), and bout length (D) of L3 expressing *npf*-Gal4>*UAS-TrpA1* and genetic controls at 30°C. **(E-G)** Arousal threshold (E), long-term aversive memory performance (F), and short-term aversive memory performance (G) in L3 expressing *npf*-Gal4>*UAS-TrpA1* and genetic controls at 30°C. **(H,I)** Short-and long-term term aversive memory performance in L3 raised on ctrl and L.S. food. A, n=18-20 larvae; B-D, n=24-61 larvae; E, n=125-160 sleep episodes, 18 larvae per genotype; F-I, n=8 PIs (240 larvae) per genotype. One-way ANOVAs followed by Sidak's multiple comparisons tests [(A) and (E-G)]; Two-way ANOVAs followed by Sidak's multiple comparison test [(B-D)]; unpaired two-tailed Student's *t*-test [(H) and (I)].
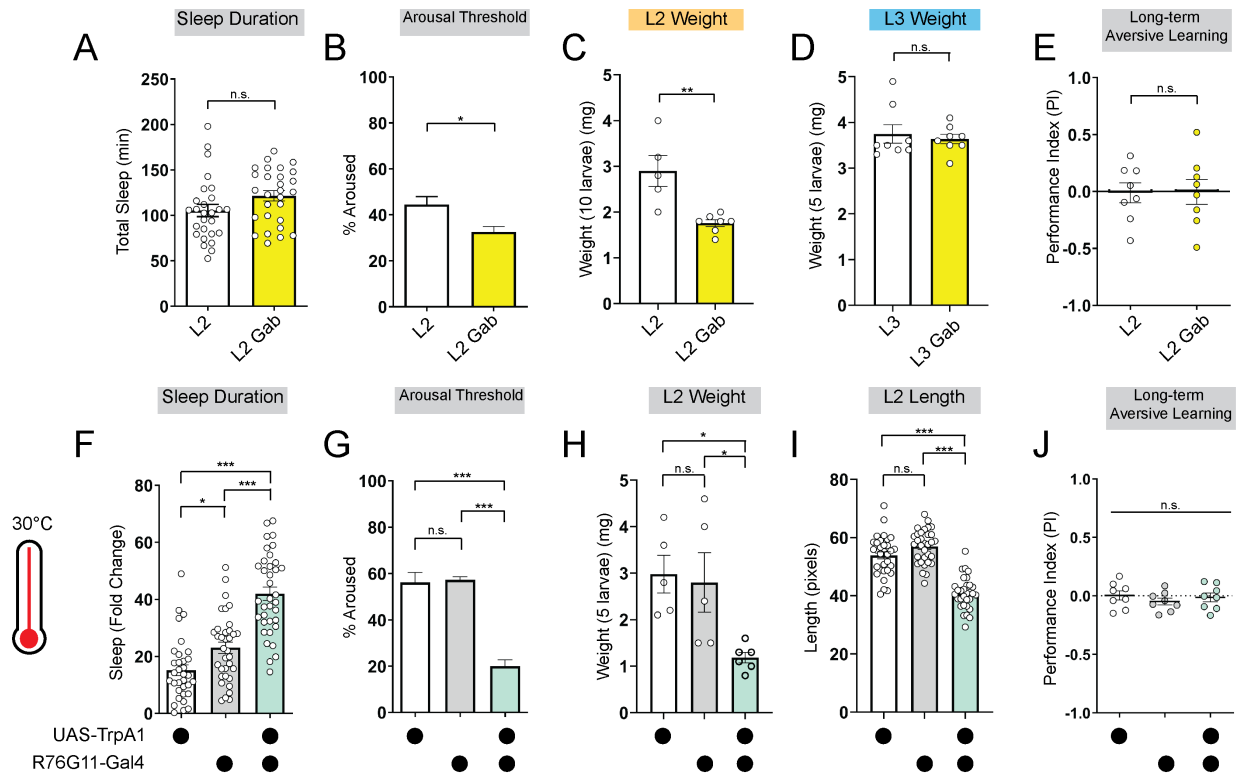
Figure 3: Deeper sleep stages in L2 are energetically disadvantageous.
(A, B) Sleep duration (A) and arousal threshold (B) of L2 control fed vehicle control (L2) or Gaboxadol (L2 Gab). **(C, D)** Total body weight of L2 (C) (in groups of 10) or L3 (D) (in groups of 5) fed vehicle control or Gaboxadol (Gab). **(E)** Long-term aversive memory performance in L2 fed vehicle control (L2) or Gaboxadol (L2 Gab). **(F, G)** Sleep duration (F) and arousal threshold (G) of L2 expressing *R76G11*-Gal4>*UAS-TrpA1* and genetic controls at 30°C. **(H, I)** Total body weight (H) and total body length (I) of L2 expressing *R76G11*-Gal4>*UAS-TrpA1* and genetic controls at 30°C. **(J)** Long-term aversive memory performance of L2 expressing *R76G11*-Gal4>*UAS-TrpA1* and genetic controls at 30°C. A, n=28 larvae; B, n=110-220 sleep episodes, 18 larvae per genotype; C, n=5-7 groups (50-70 larvae); D, n=8 groups (40 larvae); E, n=8 PIs (240 larvae) per genotype; F, n=33-36 larvae; G, n=234-404 sleep episodes, 30-40 larvae per genotype; H, n=5 groups (25 larvae); I, n=31-32 larvae; J, n=8 PIs (240 larvae) per genotype. Unpaired two-tailed Student's *t*-tests [(A-E)]; one-way ANOVAs followed by Sidak's multiple comparisons tests [(F-J)].
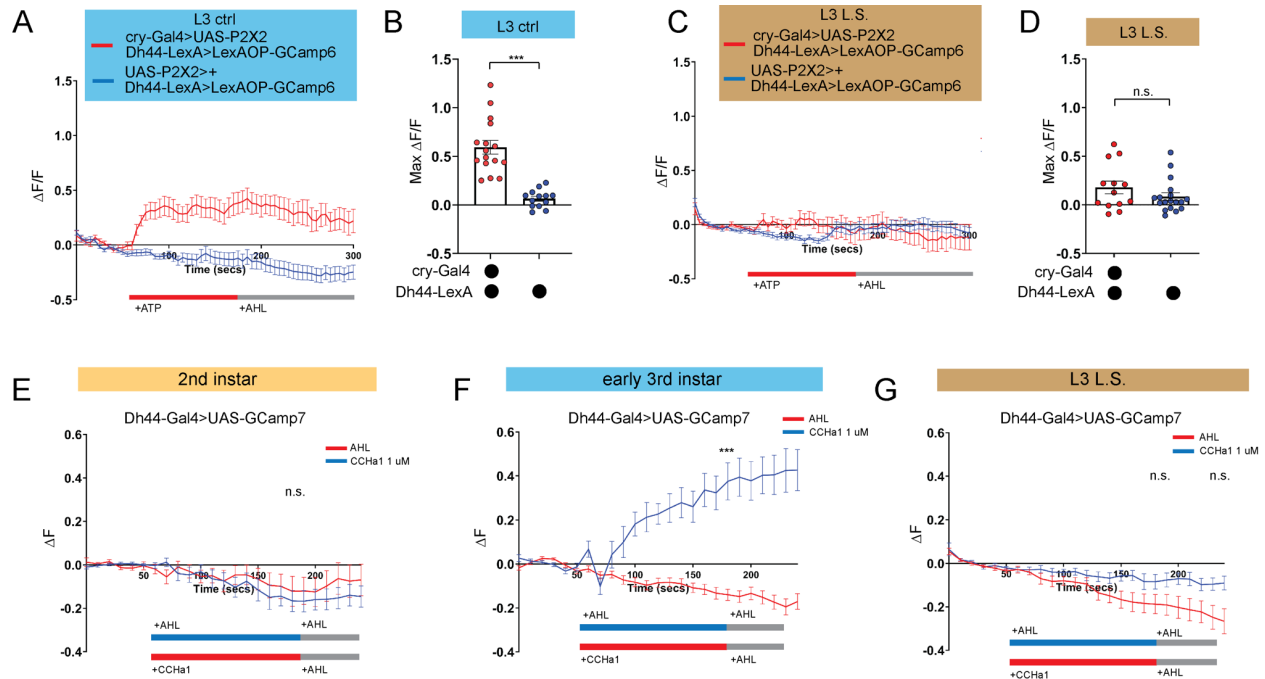
Figure 4: DN1a-Dh44 circuit formation is developmentally plastic.
(A, C) GCaMP6 signal in Dh44 neurons with activation of DN1a neurons in L3 controls (A) and L3 raised on L.S. food (C). Red bar indicates ATP application and gray bar indicates AHL application. **(B, D)** Maximum GCaMP change (ΔF/F) for individual cells in L3 controls (B) and L3 raised on L.S. food (D). **(E-G)** GCaMP7 signal in Dh44 neurons during bath application of 1 µM CCHa1 synthetic peptide in L2 (E), L3 controls (F) and L3 raised on L.S. food (G) brains. Red/blue bar indicates timing of CCHa1 (red) or buffer (AHL, blue) application and gray bar indicates timing of washout AHL application. A-D, n=12-18 cells, 8-10 brains; E-G, n=11-15 cells, 5-10 brains. Unpaired two-tailed Student's *t*-tests [(B) and (D)]; Mann-Whitney U test [(E-G)].
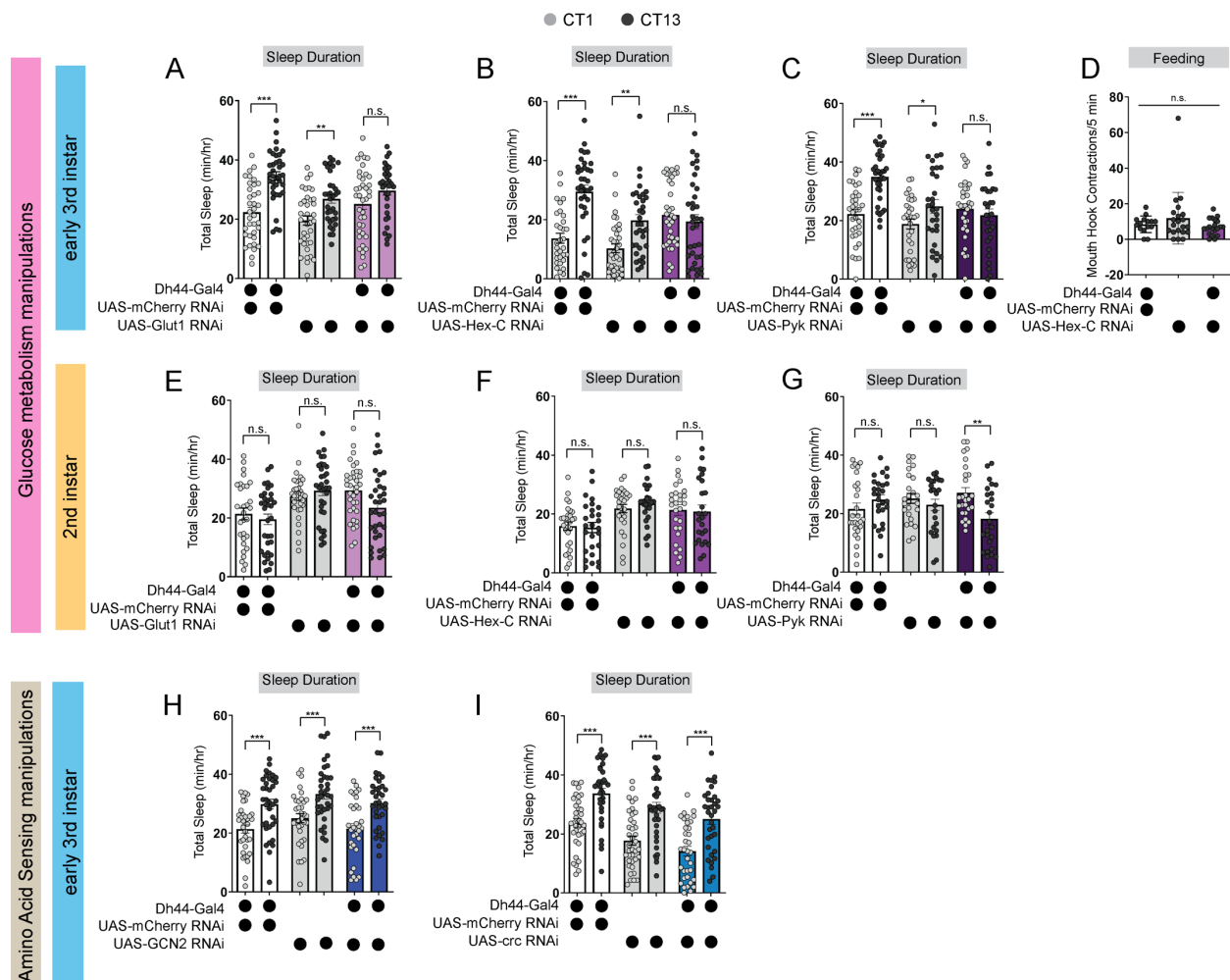
Figure 5: Dh44 neurons require glucose metabolic genes in L3 to regulate sleep-wake rhythms.
(A-C) Sleep duration in L3 expressing *UAS-Glut1-RNAi* (A), *UAS-Hex-C-RNAi* (B), and *UAS-Pyk-RNAi* (C) with *Dh44-Gal4* and genetic controls at CT1 and CT13. **(D)** Feeding rate (# of mouth hook contractions per 5 min) of L3 expressing *UAS-Hex-C-RNAi* with *Dh44-Gal4* and genetic controls at CT13. **(E-G)** Sleep duration in L2 expressing *UAS-Glut1-RNAi* (E), *UAS-Hex-C-RNAi* (F), and *UAS-Pyk-RNAi* (G) with *Dh44-Gal4* and genetic controls at CT1 and CT13. **(H, I)** Sleep duration in L3 expressing *UAS-GCN2-RNAi* (H) and *UAS-crc-RNAi* (I) with *Dh44-Gal4* and genetic controls at CT1 and CT13. A-C, n=32-40 larvae; D, n=20 larvae; E-I, n=32-40 larvae. Two-way ANOVAs followed by Sidak's multiple comparison test [(A-C) and (E-I)]; One-way ANOVAs followed by Sidak's multiple comparisons tests [(D)].
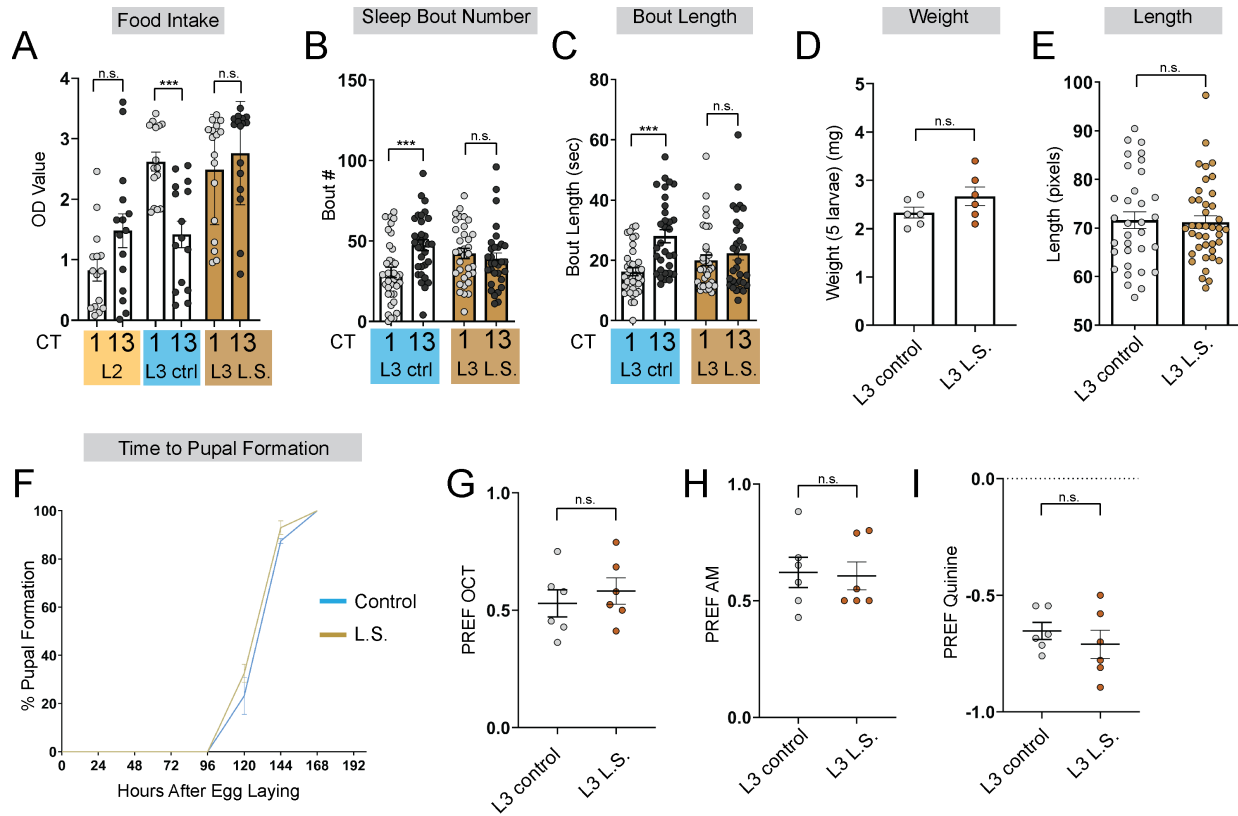
Supplemental Figure 1: Larvae on low sugar diets develop normally.
(A) Feeding amount of L2 controls, L3 raised on regular (ctrl) food, and L3 raised on low sugar (L.S.) food at CT1 and CT13. **(B, C)** Sleep bout number (B) and bout length (C) at CT1 and CT13 in L3 raised on regular (ctrl) and L.S. food. **(D)** Total body weight of early L3 (in groups of 5) raised on ctrl or L.S. food. **(E)** Total body length of early L3 raised on ctrl or L.S. food. **(F)** Developmental analysis of time to pupal formation of animals raised on ctrl or L.S. food. **(G-I)** Naïve OCT, AM, and quinine preference in L3 raised on ctrl and L.S. food. B-C, n=29-34 larvae; D, n=30 larvae per food condition; E, n=33-40 larvae; F, n=100-170 larvae; G-I, n=6 PREFs (180 larvae) per genotype. Two-way ANOVAs followed by Sidak's multiple comparison test [(B-C)]; Unpaired two-tailed Student's t-tests [(D-E) and (G-I)].
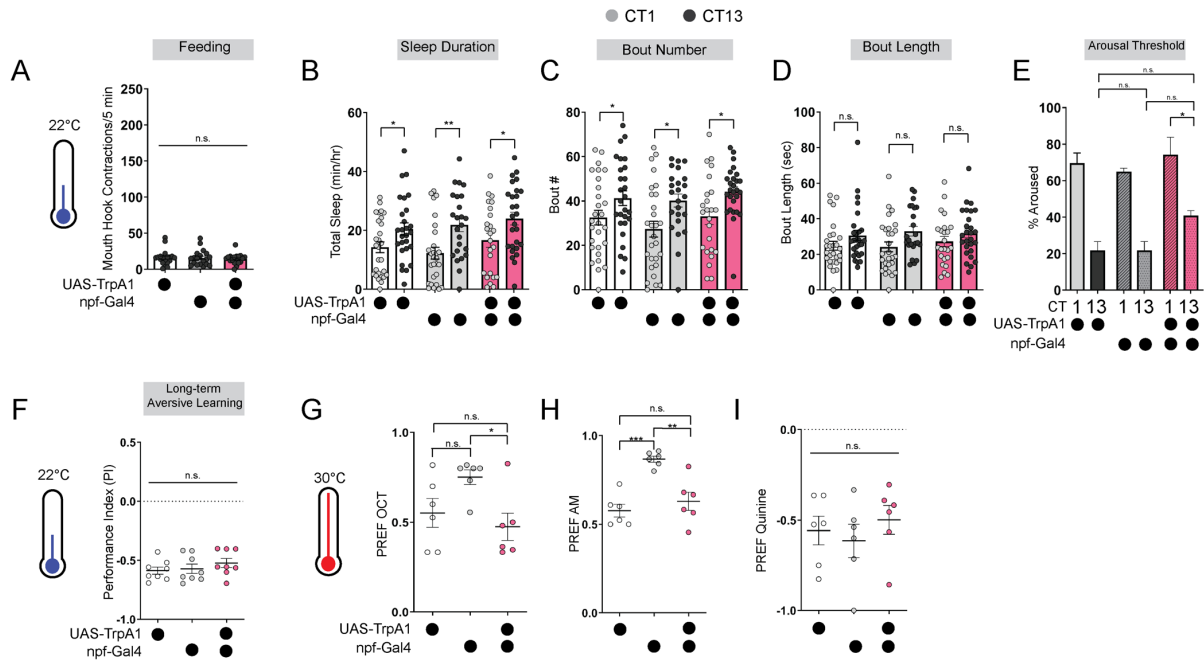
Supplemental Figure 2: Baseline odor preferences, feeding, and sleep are not affected by *npf*-Gal4 manipulations.

(A) Feeding rate of L3 expressing *npf*-Gal4>*UAS-TrpA1* and genetic controls at 22°C at CT13. **(B-E)** Sleep duration (B), bout number (C), bout length (D), and arousal threshold (E) in L3 expressing *npf*-Gal4>*UAS-TrpA1* and genetic controls at CT1 and CT13 at 22°C (temperature controls). **(F)** Long-term aversive memory performance in L3 expressing *npf*-Gal4>*UAS-TrpA1* and genetic controls at 22°C (temperature controls). **(G-I)** Naïve OCT, AM, and quinine preference in L3 expressing *npf*-Gal4>*UAS-TrpA1* and genetic controls at 30°C. A, n=18-20 larvae; B-D, n=22-27 larvae; E, n=120-205 sleep episodes, 18 larvae per genotype; F, n=8 PIs (240 larvae) per genotype; G-I, n=6 PREFs (180 larvae) per genotype. One-way ANOVAs followed by Sidak's multiple comparisons tests [(A), (E), and (F-I)]; Two-way ANOVAs followed by Sidak's multiple comparison test [(B-D)].
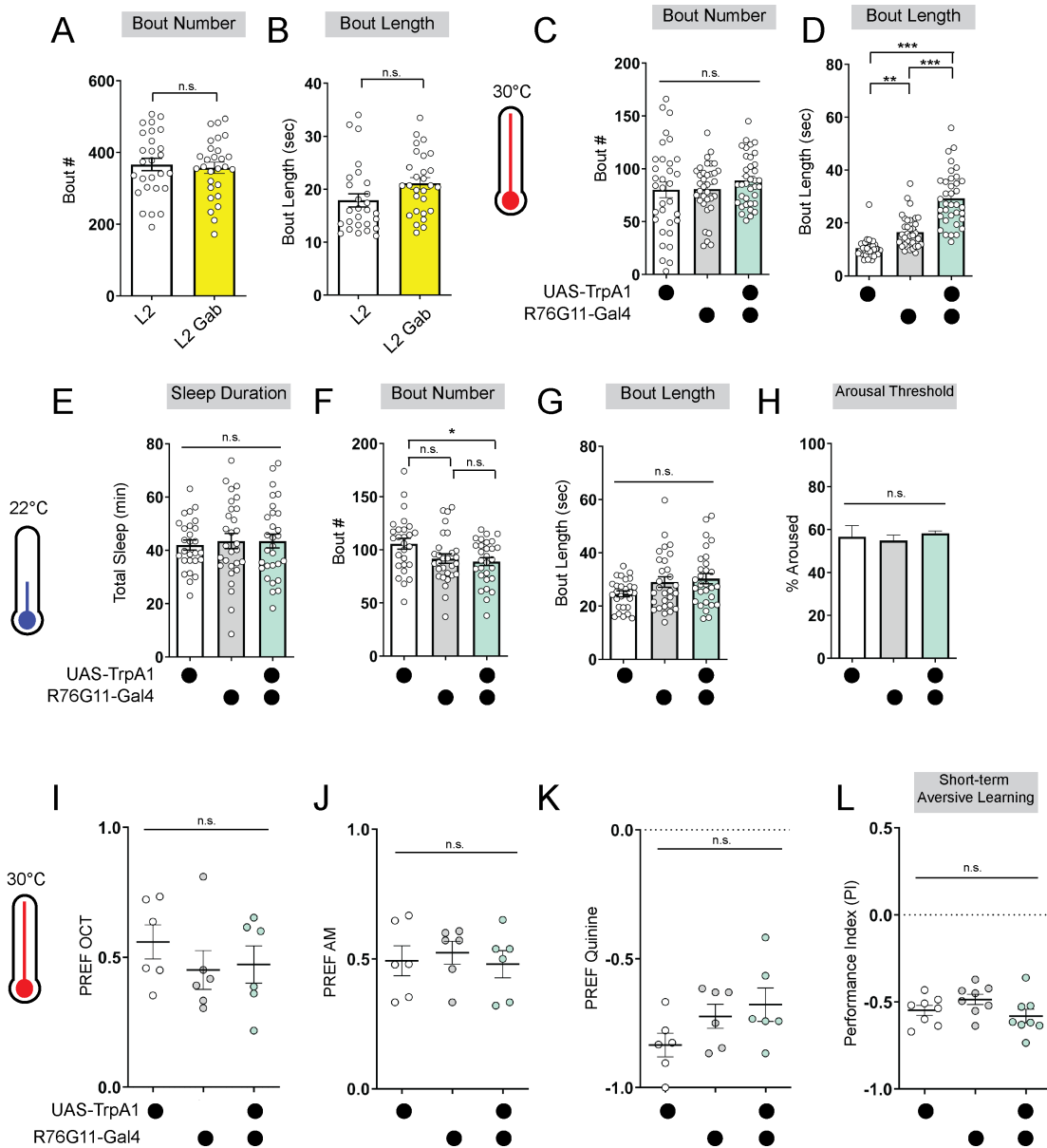
Supplemental Figure 3: Baseline sleep and odor preferences are not disrupted by *R76G11*-**Gal4 manipulations.**

(A, B) Sleep bout number (A) and bout length (B) of L2 control fed vehicle control (L2) or Gaboxadol (L2 Gab). **(C, D)** Sleep bout number (C) and bout length (D) of L2 expressing *R76G11*-Gal4>*UAS-TrpA1* and genetic controls at 30°C. **(E-H)** Sleep duration (E), bout number (F), bout length (G), and arousal threshold (H) of L2 expressing *R76G11*-Gal4>*UAS-TrpA1* and genetic controls at 22°C (temperature controls). **(I-K)** Naïve OCT, AM, and quinine preference in L2 expressing *R76G11*-Gal4>*UAS-TrpA1* and genetic controls at 30°C. **(L)** Short-term aversive memory performance of L2 expressing *R76G11*-Gal4>*UAS-TrpA1* and genetic controls at 30°C. A, B, n=28 larvae; C-D, n=33-36 larvae; E-G, n=27-29 larvae; H, n=145-316 sleep episodes, 30-40 larvae per genotype; I-K, n=6 PREFs (180 larvae) per genotype; L, n=8

PIs (240 larvae) per genotype. Unpaired two-tailed Student's t-tests [(A-B)]; One-way ANOVAs followed by Sidak's multiple comparisons tests [(C-L)].
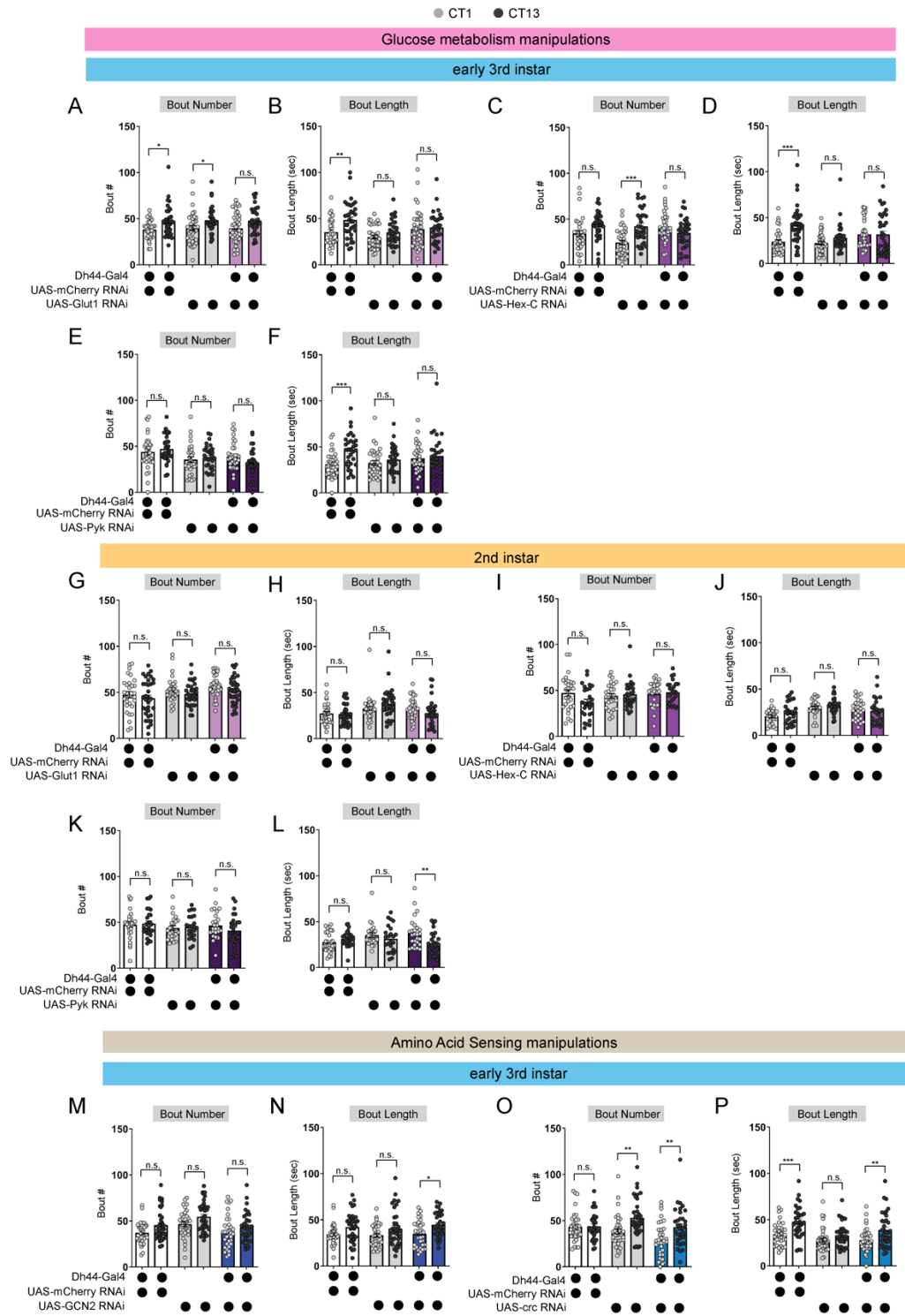
Supplemental Figure 4: Glucose metabolic gene manipulations affect L3 sleep.
(A, B) Sleep bout number (A) and bout length (B) in L3 expressing *UAS-Glut1-RNAi* with *Dh44-Gal4* and genetic controls at CT1 and CT13. **(C, D)** Sleep bout number (C) and bout length (D) in L3 expressing *UAS-Hex-C-RNAi* with *Dh44-Gal4* and genetic

controls at CT1 and CT13. **(E, F)** Sleep bout number (E) and bout length (F) in L2 expressing *UAS-Glut1-RNAi* with *Dh44-Gal4* and genetic controls at CT1 and CT13. **(G, H)** Sleep bout number (G) and bout length (H) in L2 expressing *UAS-Hex-C-RNAi* with *Dh44-Gal4* and genetic controls at CT1 and CT13. **(I, J)** Sleep bout number (I) and bout length (J) in L3 expressing *UAS-GCN2-RNAi* with *Dh44-Gal4* and genetic controls at CT1 and CT13. A-J, n=32-40 larvae. Two-way ANOVAs followed by Sidak's multiple comparison test [(A-J)].